Exceptional stiffening in composite fiber networks

A. S. Shahsavari and R. C. Picu

Department of Mechanical, Aerospace and Nuclear Engineering, Rensselaer Polytechnic Institute, Troy, New York 12180, USA

(Received 10 October 2014; revised manuscript received 13 February 2015; published 2 July 2015)

We study the small strain elastic behavior of composite athermal fiber networks constructed by adding stiffer fibers to a cross-linked base network. We observe that if the base network is in the affine deformation regime, the composite behaves similar to a fiber-reinforced continuum. When the base network is in the nonaffine deformation regime, the stiffness of the composite increases by orders of magnitude upon the addition of a small fraction of stiff fibers. The increase is not gradual, but rather occurs in two steps. Of these, one is associated with the stiffness percolation of the network of added fibers. The other, which occurs at very small fractions of stiff fibers, is due to the percolation of perturbation zones, or "interphases," induced in the base network by the stiff fibers, regions where the energy is stored mostly in the axial deformation mode. Their size controls the stiffening transition and depends on base network parameters and the length of added fibers. It is also shown that the perturbation field introduced in the base network by the presence of a stiff fiber is much longer ranged than in the case when the fiber is tied to a continuum of same modulus with the base network.

DOI: 10.1103/PhysRevE.92.012401 PACS number(s): 62.20.F−, 87.16.Ln, 61.43.Bn, 62.20.D−

I. INTRODUCTION

Materials made from fibers are ubiquitous in everyday life. Random fiber networks are the structural component of many consumer products, baby diapers, special clothing, filters, paper of various kinds, and insulation, to name just few applications. Random fiber networks are also an essential component of most biological materials. Connective tissues are networks of fibers, whereas the cytoskeleton of eukaryotic cells is an active network of F-actin.

Most networks of interest are "composite," i.e., are made from fibers with different properties. In papers, mixtures of fibers with different lengths and stiffnesses are used to provide enhanced strength and toughness. Connective tissue is made from collagen and elastin fibers [1]. The cytoskeleton includes microtubules, which are much stiffer and longer than the F-actin filaments [2]. In all these cases, the presence of the second type of fiber imparts special properties to the composite network, above and beyond the exceptional properties exhibited by some homogeneous (made from the same type of fiber) networks [3–11]. An example is provided by some elastomeric materials whose toughness and strength increase almost by an order of magnitude when a small number of much longer filaments is cross-linked to the base molecular network [12].

The conventional view in mechanics of composites is that when a set of short fibers is embedded in a continuum matrix, the stiffness of the material increases linearly with their density [13]. As discussed here and in Ref. [14], an exceptional increase in stiffness is observed when stiff fibers are cross-linked to a base homogeneous network. The effect can be used to engineer artificial fibrous materials and may be already exploited by living organisms that need to change their stiffness in a broad range without dramatic structural changes.

To place the discussion in context, it is necessary to review several results related to athermal homogeneous networks [3,5,15] made from fibers of the same length L, cross-sectional size, and the same mechanical properties, cross-linked rigidly at all contacts. The important parameters in this system are L, the density ρ, which represents the total length of fiber per unit area, and the quantity $\lambda = \sqrt{E_f I / E_f A}$, which represents the ratio of the bending and axial stiffness of fibers. Here E_f is Young's modulus of the fiber material. It has been shown [3,5,15] that the network moduli depend on parameter $w = n^7(\lambda/L)^2$, where n is the average number of cross-links per fiber and, for filaments with circular cross sections, λ/L is the fiber aspect ratio. If cross-links are placed at all fiber intersections, $n = L/l_c$, where l_c is the mean segment length which is related to ρ through the Corte-Kallmes equation $l_c = \pi/2\rho$ [16]. For w larger than a threshold ($\approx 10^5$ [15,17]), network deformation is approximately affine and similar to the deformation of a homogeneous continuum. The elastic moduli become independent of w and scale linearly with ρ and the axial stiffness of fibers $E_f A$, $E \sim E_f A \rho$. Office paper and all heavily cross-linked and high density networks belong to this category. For smaller w values, the deformation of the network is strongly nonaffine. The mechanical heterogeneity is large, and the network cannot be mapped to a homogeneous continuum model [17,18]. The elastic modulus of such two-dimensional (2D) structures scales as $E \sim E_f I \rho n^7 \sim E_f I \rho^8$ in this regime. Most biological networks belong to this class. To give an example of how fast a nonaffine network stiffens, if ρ increases by 5%, E increases by 47.7%.

Composite networks, constructed by adding fibers of certain properties set to a base homogeneous network made from different fibers, have been studied only recently [14,19,20]. Bai *et al.* [14] observed a strong gradual stiffening upon adding a small fraction of stiff fibers to a nonaffinely deforming base network, even though the added fibers do not form a secondary stress bearing network. They associate the effect with a crossover to the affine regime induced by the addition of the stiffer fibers. This small strain effect is not observed in Ref. [19] where a similar type of network is analyzed in three dimensions. However, Ref. [19] indicates that the presence of stiffer fibers reduces the critical strain marking the transition between the linear and the nonlinear elastic regimes, which is apparently in agreement with the experimental results reported

*Corresponding author: picuc@rpi.edu

in Ref. [21]. In this paper, we consider a family of composite networks similar to those studied in Ref. [14] and show that stiff fibers bonded to a nonaffinely deforming base induce an "interphase" (i.e., a region of the base network) in which the strain energy is stored predominantly in the axial mode of the fibers. These interphases are approximately elliptical with their large semiaxis scaling with the length of the added fibers and their small semiaxes being defined by the base network density and fiber length. When these interphases percolate, the stiffness of the composite increases dramatically. This happens at a density of added fibers significantly smaller than that at which the added fibers percolate and form a stress bearing network. Hence, we show that the stiffening observed in Ref. [14] happens abruptly at a well-defined density of added fibers due to a percolation phenomenon.

II. MODEL DEFINITION AND METHODS

To construct a two-dimensional network model (Mikado), one drops fibers of length L with random centroid positions and random orientations in a domain of size a. The density ρ is kept as a parameter. Fibers are elastic with modulus E_f and have axial and bending stiffnesses $E_f A$ and $E_f I$, respectively. Here we denote the base and added stiff fibers by subscripts "b" and "a," respectively. The added fibers are introduced with random centroid positions and random orientations. These are cross-linked to all fibers they contact, base and added, or are cross-linked only to the base fibers, in separate models. The two types of networks are referred to as "fully cross-linked" (FCL) and "base cross-linked" (BCL), respectively. The fibers belonging to the base are cross-linked at all contact points. All cross-links are rigid such that they transmit both forces and moments.

Fibers are represented as Timoshenko beams with the strain energy computed as indicated in Ref. [22]. Specifically, the total energy of the system is the sum of the strain energies associated with bending, axial, and shear deformation, i.e.,

$$U = \frac{1}{2}\sum_{\text{fibers}} \int E_f I\left(\frac{d\psi(s)}{ds}\right)^2 + E_f A\left(\frac{du(s)}{ds}\right)^2 + \gamma G_f A\left(\frac{dv(s)}{ds} - \psi(s)\right)^2 ds. \quad (1)$$

In this expression $v(s)$ represents the transverse displacement, and $\frac{du(s)}{ds}$ is the axial strain at position s along the fiber. The rotation of the fiber cross section is $\frac{dv(s)}{ds}$, whereas $\psi(s)$ represents the rotation of a plane which remains perpendicular to the neutral axis of the beam. Hence $\frac{dv(s)}{ds} - \psi(s)$ represents the shear deformation of the beam. γ is a constant which is considered 0.88 (for beams with circular cross sections).

Due to the pronounced heterogeneity of the network which is introduced by the random process of network generation, the overall mechanical response is affected by strong size effects [17]. In this paper we consider systems large enough to eliminate the size effects and to render the computed effective moduli independent of the boundary conditions ($a > 10L$).

The network is deformed in uniaxial tension. Displacement boundary conditions are applied in the direction of loading $u_2 = \delta$, whereas the boundaries parallel to the loading direction are traction free, $\sigma_{11} = 0; \sigma_{12} = 0$. Periodic boundary conditions are used in all models. The solution is found by minimizing the total system energy using the finite element solver ABAQUS.

Added fibers of length ranging from $L_a = 0.25$ to 1.5 and with $\lambda_a = 10^{-2}$ are considered. Unless otherwise specified, the base network has $L_b = 0.5$, $\rho_b = 50$ and λ_b in the range $(10^{-7}, 10^{-4})$ and has cross-links at all fiber intersection points. All lengths are normalized with an arbitrary length equal to twice the base fiber length. The base network with $\lambda_b = 10^{-7}$ is strongly nonaffine, and the degree of nonaffinity decreases gradually as λ_b increases.

III. RESULTS

Let us focus first on the overall behavior of the composite network and its relationship with the relevant system parameters. Figure 1 shows the variation in the network modulus E with the density of added fibers ρ_a for base networks with $\lambda_b = 10^{-4}, 10^{-5}, 10^{-6}$, and 10^{-7}. FCL cases are shown with open symbols and dashed lines, whereas BCL cases are shown with filled symbols and continuous lines. The data points on the vertical axis correspond to the homogeneous base network and can be predicted based on the results reported in Refs. [15,22].

In the FCL case, the data merge to a unique curve at large ρ_a since in this limit the network formed by the added fibers dominates the behavior. This limit configuration corresponds to a homogeneous network with $L_a = 0.5$ and $\lambda_a = 10^{-2}$. The FCL composites with $\lambda_b < 10^{-4}$ exhibit a significant increase in the stiffness at $\rho_{a_2} \approx 12$, which corresponds to the stiffness percolation of the added network. The transition is not observed when the added fibers are not cross-linked between themselves (BCL), which indicates that this is indeed a stiffness percolation point. The critical point for stiffness percolation in this model is defined by $L_a \rho_{a_2} = 6.7$ [23,24], which corresponds to $\rho_{a_2} \approx 13.4$. The value observed in Fig. 1 is slightly smaller, likely due to the size effect. The size effect,

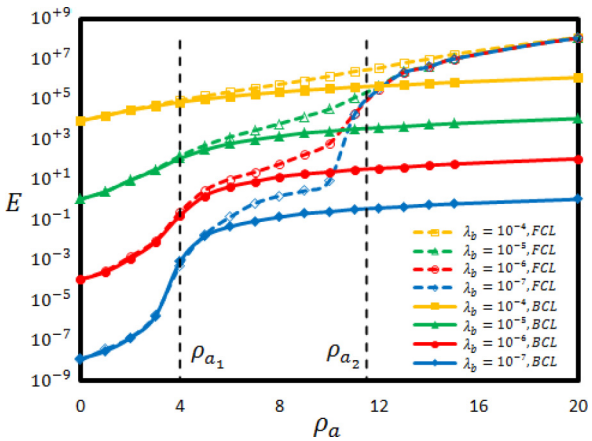

FIG. 1. (Color online) Composite network modulus versus the density of stiff added fibers ρ_a. The added fibers have $L_a = 0.5$, $\lambda_a = 10^{-2}$, whereas the base has $L_b = 0.5$, $\rho_b = 50$, and various λ_b's. FCL and BCL cases are shown with dashed and continuous lines, respectively. Two transitions are observed for the more nonaffinely deforming networks at critical densities ρ_{a_1} and ρ_{a_2}.

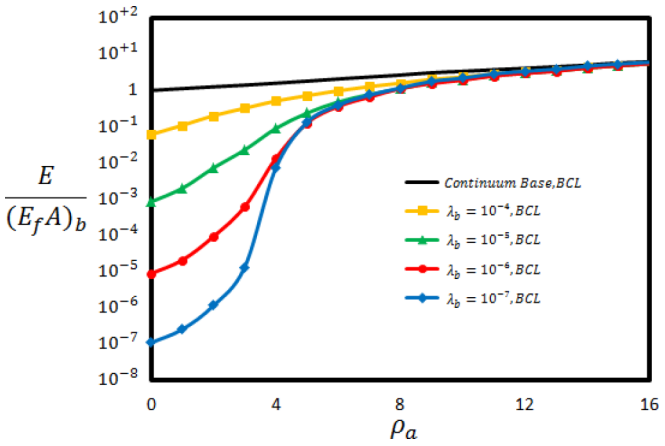

FIG. 2. (Color online) BCL data from Fig. 1 replotted with the vertical axis normalized by $(E_f A)_b$ to evidence the parameter controlling the behavior at large ρ_a. For the curve corresponding to the continuum base, the vertical axis is normalized with the modulus of the continuum.

which is particularly strong close to the critical point, renders the percolation transition rather gradual.

Interestingly, the curves corresponding to the lower value of λ_b, i.e., $\lambda_b = 10^{-6}$ and $\lambda_b = 10^{-7}$, exhibit another transition at much smaller densities of the added fibers $\rho_{a_1} \approx 4$. In this range of densities, the "stiffeners" are too sparse to contact each other. This sharp transition was not observed in Ref. [14] due to their choice of added fiber length L_a as discussed below.

The BCL systems exhibit the transition at ρ_{a_1} but not the percolation transition at ρ_{a_2}. In the limit of large ρ_a clear differences are observed between the asymptotes. However, all curves are parallel and depend on ρ_a. To clarify the origin of this difference, the BCL curves from Fig. 1 are replotted in Fig. 2 with the vertical axis normalized by the axial stiffness of the base network fibers $(E_f A)_b$. The collapse of the curves at large ρ_a indicates that in this limit the stiffness of BCL networks scales as $E \sim (E_f A)_b$.

The added fibers of these networks are connected via the base fibers. As the density ρ_a increases, the length of a segment (or path) belonging to the base network which connects two added fibers decreases. This situation is akin to the systems studied in Refs. [25,26] where homogeneous networks with flexible cross-links are studied. As the stiffness of the cross-links decreases, the network behavior is controlled by these connectors, and the modulus decreases linearly with their stiffness. In our case, the connectors are segments of the base network fibers. As these become shorter, their behavior is controlled by their axial stiffness. This follows from the known result that the modulus of homogeneous networks with short fiber segments between cross-links is proportional to the axial stiffness of fibers $E \sim E_f A$. Hence, the presence of a small number of stiff fibers leads to a crossover to the axially dominated and affine deformation mode of the network. Note that this transition happens in homogeneous networks at much larger densities. To reemphasize the effect, we show in Fig. 2 results for systems in which the stiff fibers are bonded to a continuum (which plays the role of the base in this case). The computed stiffness is normalized by the modulus of the continuum base. This situation corresponds to a perfectly affinely deforming base and represents the limit of the series of base networks with increasing λ_b. The spectacular difference between this curve and those corresponding to bases having small λ_b values evidences the strong constraining effect of the stiff added fibers on the nonaffine deformation of the base network.

The most interesting result of the present data set is the rapid increase in the stiffness close to the critical density ρ_{a_1}. Therefore, it is necessary to clarify the origin of this phenomenon which is not encountered in continuum equivalents of this problem. To this end, we study the perturbation field induced by an isolated added fiber to the deformation field of the base network. We place a single stiff fiber on a nonaffine base of $\lambda_b = 10^{-6}$, $\rho_b = 50$, and $L_b = 1.0$ and subject the system to uniaxial deformation in a direction making 45° with the fiber axis. We evaluate ratio $\mathcal{R}$ of the strain energy of the base network stored in the axial deformation mode to the total strain energy. The homogeneous base network is in the bending dominated regime, and $\mathcal{R}$ is smaller than 0.05 for all regions of this system. Figure 3 shows the map of $\mathcal{R}$ for the base network with a single added fiber. The map indicates that a perturbed region, which we refer to as an interphase, exists around the stiffener. Within this approximately elliptical interphase, $\mathcal{R}$ takes values as large as 0.5. The result shown in Fig. 3 is obtained by averaging over 20 replicas of the base network in order to reduce the noise, but the effect is visible in each realization.

Systems having the same base network and added fibers of length varying from $L_a = 0.25$ to 3 are also studied, and we observe that the large semiaxis of the elliptical interphase is proportional to L_a. The small semiaxis is independent of L_a and is defined by the parameters of the base network. Specifically, it increases with increasing L_b and ρ_b. The

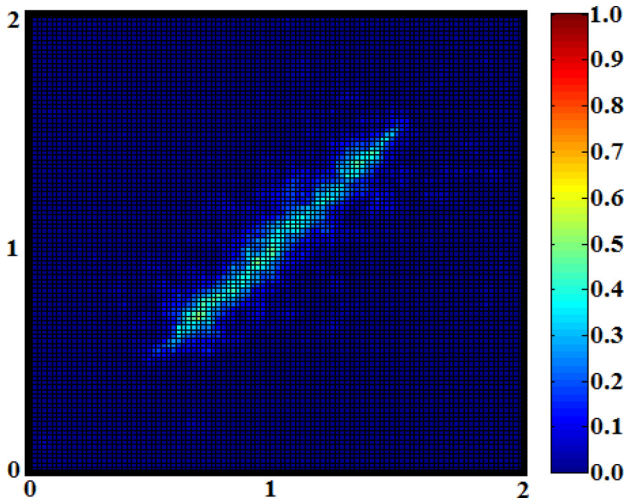

FIG. 3. (Color online) Map of the fraction $\mathcal{R}$ of the strain energy stored in the axial deformation mode of fibers to the total strain energy for a base network with $L_b = 0.5, \rho_b = 50$, and $\lambda_b = 10^{-6}$ to which a single fiber with $L_a = 1.5$, $\lambda_a = 10^{-2}$ is added. The fiber is oriented at 45° relative to the (vertical) loading direction. The energy stored in the added fiber is not included in the values reported here.

dependence can be approximated with a linear function in the range studied $\rho_b \in [50,100], L_b \in [0.5,1.5]$.

To further investigate this effect, added fibers of different lengths are considered, and the analysis leading to the BCL data in Fig. 2 is repeated. Specifically, base networks with $\rho_b = 50$ and λ_b ranging from 10^{-7} to 10^{-4} and added fibers with $L_a = 0.25$, 0.5, and 1 and $\lambda_a = 10^{-2}$ are considered in different models. The modulus of these composites normalized with $(E_f A)_b$ is shown in Fig. 4(a) versus ρ_a. The critical density ρ_{a_1} decreases with increasing L_a.

Let us consider now that the large increase in stiffness at ρ_{a1} and the crossover of the system to the axial deformation mode are associated with the percolation of the added fiber interphases. To quantify this effect, we make use of percolation data for identical, randomly distributed, and randomly oriented overlapping ellipses in 2D reported in Refs. [27,28]. If the semiaxes of the ellipses are s_1 and $s_2 (s_1 > s_2)$, the percolation threshold can be approximated by $\rho_{a_1}(2s_1) \simeq -\frac{4}{\pi}\ln\frac{18}{19+4y}$, where $y = s_1/s_2 + s_2/s_1$ [27]. The right side of this equation is shown graphically in Fig. 5. The plot also shows $\rho_{a_1}(2s_1)\sqrt{s_2/s_1}$ versus s_2/s_1, which is approximately constant over a broad range of the aspect ratio. Hence, the quantity $\rho_{a_1}(2s_1)$ can be approximated up to a multiplicative constant with $\sqrt{s_1/s_2}$. The approximation is valid for almost the entire

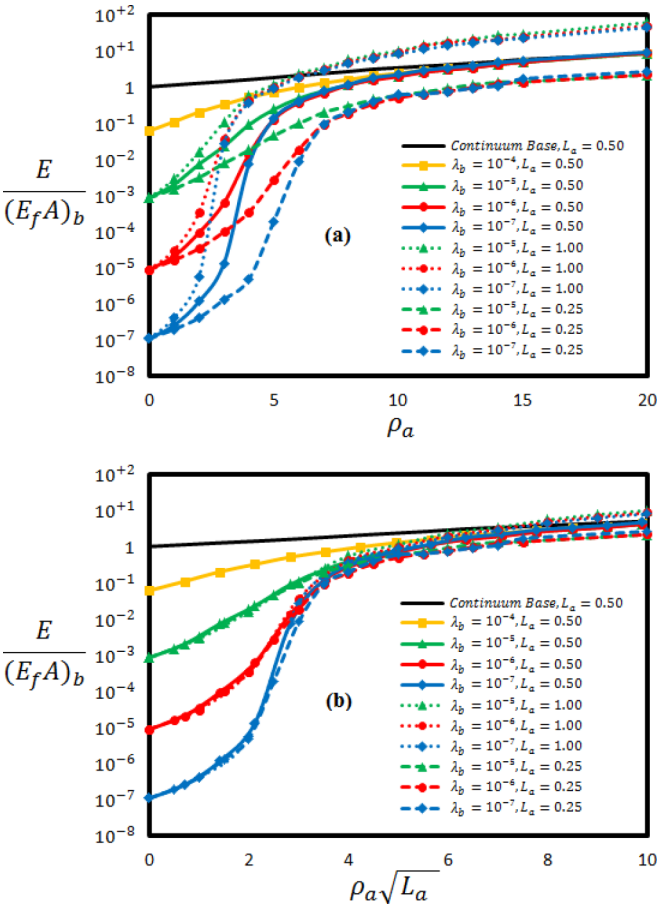

FIG. 4. (Color online) BCL results for cases in which the length of the added fibers L_a is varied. (a) shows the data in coordinates similar to those in Fig. 2. The plot in (b) uses a different variable on the horizontal axis such to collapse the curves at the transition ρ_{a_1}.

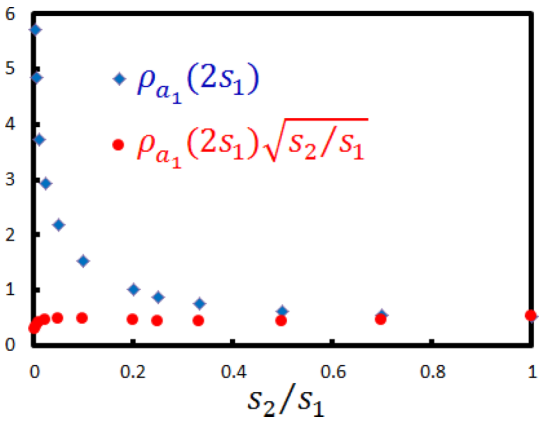

FIG. 5. (Color online) Variation in the normalized number density of ellipses at percolation with the ellipse aspect ratio (blue squares) along with the variation of the same function multiplied by $\sqrt{s_2/s_1}$ (red circles).

range of aspect ratios, i.e., for $0.01 < s_2/s_1 < 1$. With $s_1 \sim L_a$, we conclude that $\rho_{a_1}\sqrt{L_a}$ should be a constant for a given base (i.e., for constant s_2). Figure 4(b) shows the curves in Fig. 4(a) with the variable on the horizontal axis modified to $\rho_a\sqrt{L_a}$. The figure shows the collapse of the stiffening transitions of networks with different added fibers and statistically identical bases.

To check the robustness of these concepts, we repeated the analysis leading to the data in Fig. 4 with base networks with $\rho_b = 100$, $\lambda_b = 10^{-6}$, and $L_b = 0.5$ and with $\rho_b = 50$, $\lambda_b = 10^{-6}$, and $L_b = 1$ in separate simulations. The results are shown in Figs. 6(a) and 6(b), respectively. The parameters of the added fibers are similar to those used in Fig. 4, i.e., $\lambda_a = 10^{-2}$ and $L_a = 0.25$, 0.5, or 1 in separate models. The curves collapse in the vicinity of the critical point ρ_{a_1}, indicating that the model proposed holds for various bases as well. We also note that a similar result can be obtained if the interphase shape is considered rectangular and percolation data for identical overlapping rectangles are used [29]. The present conclusions hold provided L_a is sufficiently large (L_a larger than the mean segment length of the base network) such that the added fibers effectively reinforce the base network.

It is interesting to draw a parallel between the role of interphases in this problem and in polymer-based nanocomposites. It is now commonly accepted that the polymer matrix in the vicinity of inclusions has modified properties relative to the polymer far from such interfaces. This interphase plays a critical role in nanocomposites since as the filler size decreases, the interphase volume, which scales with the filler-matrix interface area, increases fast. The macroscopic properties of the composite become then dominated by the properties of these interphases, and interesting properties result when the interphases percolate. This is similar to the case discussed here in which the modification of the base network behavior due to the added fibers becomes visible on the system scale only after the percolation of interphases, point beyond which it has a dramatic global effect.

It is further interesting to outline a related effect which leads to enhanced long-range interaction of the added stiff fibers. Let us study the perturbation field induced by an isolated

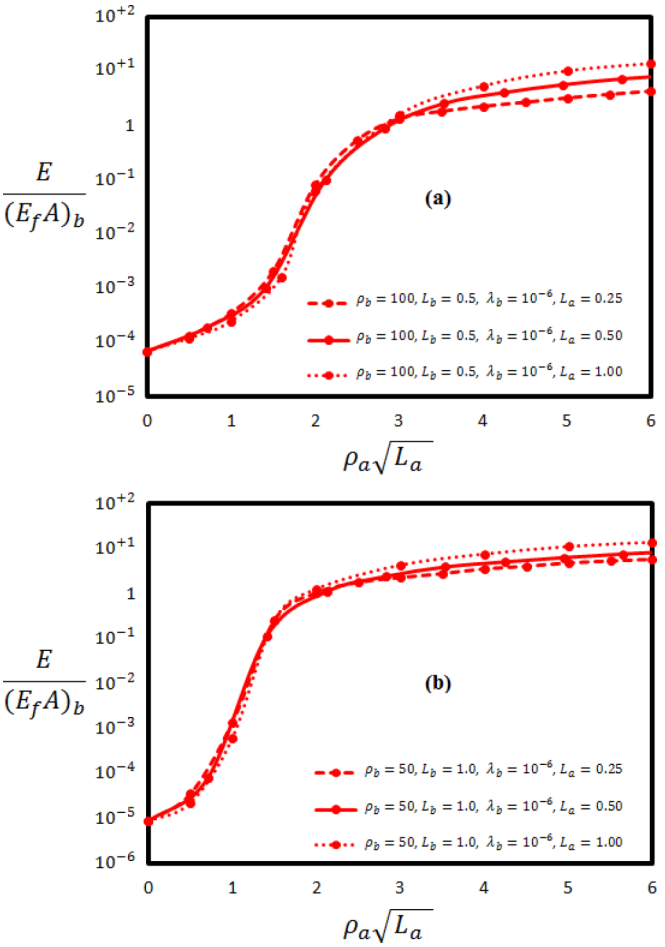

FIG. 6. (Color online) BCL results for cases in which the length of the added fibers L_a is varied and nonaffinely deforming networks with different fiber length L_b and different density ρ_b are considered as bases [(a) and (b), respectively].

added fiber in the deformation field of the base network. As described above, we place a single stiff fiber on a nonaffine base of $\lambda_b = 10^{-6}$ and $\rho_b = 50$ and subject the system to uniaxial deformation in a direction making 45° with the fiber axis. The perturbation field is computed by subtracting the displacements of the network without the added fiber, and the result is averaged over ten realizations of the base network to eliminate the variability introduced by the specific base network geometries.

Figure 7(a) shows the normalized perturbation displacement $\Delta u_2 = (u_2 - u_2^b)/\delta$ introduced by an added fiber of length $L_a = 0.5$ and $\lambda_a = 10^{-2}$. u_2 and u_2^b are the displacement fields of the base cross-links with and without the added fiber in the direction of the far-field loading x_2, and δ is the applied boundary displacement. Figure 7(b) shows the equivalent field computed for the case when the same fiber is tied to a continuum base of stiffness equal to that of the base network used to compute u_2^b in Fig. 7(a). The number of contours in the two figures is identical, and the contours correspond to the same values of the variable.

The figure indicates a substantial difference between the range and the amplitude of the effect of a stiffener fiber added to the network and to a continuum of the same effective stiffness. The fiber added to the network modifies the deformation of the base network to a much larger extent. Clearly, this is another manifestation of the interphase discussed above and contributes to the enhanced interaction of stiffener fibers causing the effect shown in Fig. 1.

To summarize the above discussion, exceptional stiffening results in composite networks constructed by adding relatively stiff fibers to a nonaffinely deforming homogeneous network. Multiple orders of magnitude increase in stiffness is observed for the network with $\lambda_b = 10^{-7}$ upon the addition of only 5% of fibers with $\lambda_a = 10^{-2}$ (Fig. 1). This is in sharp contrast with the increase of 47.7% expected for a nonaffinely deforming homogeneous network whose density is increased by 5%

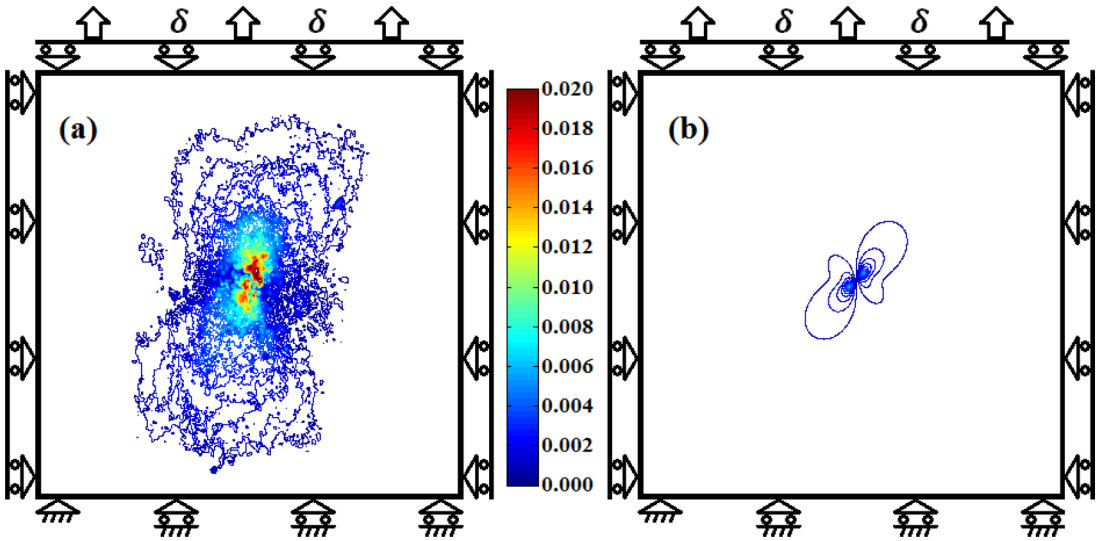

FIG. 7. (Color online) Perturbation field $\Delta u_2/\delta$ introduced by cross-linking a stiff fiber with $L_a = 0.5$, $\lambda_a = 10^{-2}$ to (a) a nonaffine base network with $\rho_b = 50$ and $\lambda_b = 10^{-6}$ and (b) to a continuum of stiffness identical to that of the base network in (a). The perturbation field is normalized with δ, the applied far-field displacement. The fiber is oriented at 45° relative to the (vertical) loading direction.

(equivalent to adding fibers identical to those of the base) and with the small 5% increase expected for an affinely deforming homogeneous network whose density increases by 5%.

IV. CONCLUSIONS

In this paper we investigate the variation in the elastic modulus of a fiber network to which much stiffer fibers are bonded and show that an exceptionally strong stiffening effect is observed at small densities of stiffener fibers. It is shown that the effect is associated with the percolation of regions in which the deformation of the base network is perturbed by the presence of added stiff fibers and this occurs at densities ρ_{a_1} smaller than required to form a stress bearing network of added fibers (ρ_{a_2}). The difference between ρ_{a_1} and ρ_{a_2} depends primarily on the length of added fibers L_a. This percolation transition is observed in both FCL and BCL networks. The perturbation field introduced by an isolated stiff fiber tied to a nonaffinely deforming network does not have a continuum equivalent. Hence, the observed large sensitivity of the effective modulus to the addition of a small number of stiff fibers is not observed in affinely deforming networks and when fibers are bonded to continua. The present results indicate how a network can be engineered to take advantage of this large sensitivity. This effect may be already used by living organisms to modify their properties in a broad range with minimal structural changes.

[1] S. C. Cowin and S. B. Doty, *Tissue Mechanics* (Springer, New York, 2006).
[2] D. A. Fletcher and R. D. Mullins, Nature (London) **463**, 485 (2010).
[3] D. A. Head, A. J. Levine, and F. C. MacKintosh, Phys. Rev. E **68**, 061907 (2003).
[4] C. P. Broedersz, M. Sheinman, and F. C. MacKintosh, Phys. Rev. Lett. **108**, 078102 (2012).
[5] R. C. Picu, Soft Matter **7**, 6768 (2011).
[6] C. P. Broedersz, X. Mao, T. C. Lubensky, and F. C. MacKintosh, Nat. Phys. **7**, 983 (2011).
[7] O. Lieleg, M. M. A. E. Claessens, and A. R. Bausch, Soft Matter **6**, 218 (2010).
[8] K. E. Kasza, G. H. Koenderink, Y. C. Lin, C. P. Broedersz, W. Messner, F. Nakamura, T. P. Stossel, F. C. MacKintosh, and D. A. Weitz, Phys. Rev. E **79**, 041928 (2009).
[9] T. van Dillen, P. R. Onck, and E. van der Giessen, J. Mech. Phys. Solids **56**, 2240 (2008).
[10] M. L. Gardel, J. H. Shin, F. C. MacKintosh, L. Mahadevan, P. Matsudaira, and W. A. Weitz, Science **304**, 1301 (2004).
[11] G. A. Buxton and N. Clarke, Phys. Rev. Lett. **98**, 238103 (2007).
[12] M. Y. Tang and J. E. Mark, Macromolecules **17**, 2616 (1984).
[13] G. J. Dvorak, *Mechanics of Composite Materials* (Springer, New York, 2013).
[14] M. Bai, A. R. Missel, W. S. Klung, and A. J. Levine, Soft Matter **7**, 907 (2011).
[15] A. S. Shahsavari and R. C. Picu, Philos. Mag. Lett. **93**, 356 (2013).
[16] O. Kallmes and H. Corte, Tappi J. **43**, 737 (1960).
[17] A. S. Shahsavari and R. C. Picu, Int. J. Solids Struct. **50**, 3332 (2013).
[18] H. Hatami-Marbini and R. C. Picu, Phys. Rev. E **80**, 046703 (2009).
[19] E. M. Huisman, C. Heussinger, C. Storm, and G. T. Barkema, Phys. Rev. Lett. **105**, 118101 (2010).
[20] H. Wada and Y. Tanaka, Europhys. Lett. **87**, 58001 (2009).
[21] Y. C. Lin, G. H. Koenderink, F. C. MacKintosh, and D. A. Weitz, Soft Matter **7**, 902 (2011).
[22] A. S. Shahsavari and R. C. Picu, Phys. Rev. E **86**, 011923 (2012).
[23] J. Wilhelm and E. Frey, Phys. Rev. Lett. **91**, 108103 (2003).
[24] M. Latva-Kokko and J. Timonen, Phys. Rev. E **64**, 066117 (2001).
[25] G. Zagar, P. R. Onck, and E. van der Giessen, Macromolecules **44**, 7026 (2011).
[26] C. P. Broedersz, C. Storm, and F. C. MacKintosh, Phys. Rev. Lett. **101**, 118103 (2008).
[27] W. Xia and M. F. Thorpe, Phys. Rev. A **38**, 2650 (1988).
[28] Y. B. Yi and A. M. Sastry, Phys. Rev. E **66**, 066130 (2002).
[29] J. Li and M. Ostling, Phys. Rev. E **88**, 012101 (2013).